ZESZYTY NAUKOWE POLITECHNIKI ŚLĄSKIEJ 2004
Seria: ELEKTRYKA z. 191 Nr kol. 1633

Dariusz SPAŁEK
Instytut Elektrotechniki Teoretycznej i Przemysłowej. Zakład Elektrotechniki i Informatyki

ELECTROMECHANICAL CONVERTERS LINEAR, CYLINDRICAL AND SPHERICAL – PART II – FORCE AND TORQUE CALCULATION

Summary. The paper deals with the problem of electromagnetic force and torque analysis for linear, cylindrical and spherical electromechanical converters taking into account region anisotropy. The electromagnetic force and torque are determined analytically with the help of separation method for each problem (part I). The results obtained can be used as test tasks for electromagnetic field, force and torque numerical calculations. The analytical relations for torque and forces are used for analysis of material parameters influence on electromechanical converter work.

PRZETWORNIK ELEKTROMECHANICZNY LINIOWY, CYLINDRYCZNY I SFERYCZNY – CZĘŚĆ II – OBLICZENIA SIŁ I MOMENTU ELEKTROMAGNETYCZNEGO

Streszczenie. Artykuł przedstawia obliczenia analityczne sił i momentów sił dla przetwornika elektromechanicznego o symetrii liniowej, cylindrycznej i sferycznej z uwzględnieniem anizotropii środowiska. Analityczne rozwiązania równań pola elektromagnetycznego uzyskano korzystając z metody separacji zmiennych (część I). Wyniki analiz mogą być wykorzystane jako zadania testowe dla analiz numerycznych. Analityczne zależności na siły i moment elektromagnetyczny wykorzystano do analizy wpływu parametrów materiałowych na pracę przetwornika elektromechanicznego.

1. INTRODUCTION

The determination of forces induced by electromagnetic field in electromechanical converter is important problem [1, 2, 3, 4]. For electromechanical converters the acting force or torque values play deciding role for users. Modern technologies enable to construct electromechanical converters with parts having wide range of properties between them anisotropic [2, 6, 8]. Especially, the induction motors – linear, cylindrical and spherically shaped have got magnetically anisotropic parts. The magnetic anisotropy could increase the value of forces and torques arising in electromechanical converter. The intention of this paper is to present the analytical solutions for electromagnetic force/torque for linear, cylindrical and

spherical induction motor problems. Basing on the main equation for electromagnetic forces density there are presented and discussed forces and torques values acting in electromechanical converters. The analytical relations for torque and forces are the base for material parameters influence analysis. The presented below solutions for anisotropic and isotropic cases for magnetic circuit of induction motor can be used as a test-tasks for numerical packages, too.

2. ELECTROMAGNETIC FIELD EQUATIONS

Electromagnetic field force volume density in curvilinear co-ordinate system can be presented with the help of Maxwell equation

$$\mathrm{curl}\vec{H} = \vec{j} + \frac{\partial \vec{D}}{\partial t}, \tag{1}$$

and Lorentz force density in the form of

$$\vec{f} = \rho\vec{E} + \vec{j} \times \vec{B}, \tag{2}$$

which constitute one component of total electromagnetic field force. Lorentz force density can be rearranged to the following form of

$$\vec{f} = \rho\vec{E} + \vec{j} \times \vec{B} = \vec{E}\,\mathrm{div}\,\vec{D} + (\mathrm{curl}\vec{H} - \dot{\vec{D}}) \times \vec{B}, \tag{3}$$

that leads to the relation

$$\vec{f} = -\frac{\partial}{\partial t}(\vec{D} \times \vec{B}) + \vec{H}\,\mathrm{div}\,\vec{B} + \mathrm{curl}(\vec{H}) \times \vec{B} + \vec{E}\,\mathrm{div}\,\vec{D} + \mathrm{curl}(\vec{E}) \times \vec{D}, \tag{4}$$

where it was added component $\vec{H}\,\mathrm{div}\,\vec{B} = 0$. The second and third component on the right-hand (4) can be written in the form of

$$\mathrm{curl}(\vec{H}) \times \vec{B} + \vec{H}\,\mathrm{div}\,\vec{B} = \vec{i}_u\,\mathrm{div}_{|u|}(H_u\vec{B}) - \mathrm{grad}(\tfrac{1}{2}\vec{H}\vec{B}) - \vec{N}_\mu + \vec{k}_\mu, \tag{5}$$

and its u-th component takes the given below form

$$(\mathrm{curl}(\vec{H}) \times \vec{B} + \vec{H}\,\mathrm{div}\,\vec{B})_u = \frac{1}{L_{|u|}}\mathrm{div}(L_{|u|}H_u\vec{B}) - \frac{\partial(\frac{1}{2}\vec{H}\vec{B})}{L_{|u|}\partial x_u} - (\vec{N}_\mu)_u + (\vec{k}_\mu)_u, \tag{6}$$

where it was denoted (indices in the form of |u| are not summarised)

$$\mathrm{div}_u(*) = \frac{1}{L_u}\mathrm{div}\{L_{|u|} \cdot (*)\}, \tag{7}$$

$$\vec{N}_\mu = \tfrac{1}{2}B_u B_w\,\mathrm{grad}(\nu_{uw}), \tag{8}$$

$$\vec{k}_\mu = -\tfrac{1}{2}\frac{B_u B_w \nu_{uw}}{L_{|u|}L_{|w|}}\mathrm{grad}(L_{|u|}L_{|w|}) \tag{9}$$

and the fact of material coefficients symmetry $\nu_{uv} = \nu_{vu}$, $\varepsilon_{uv} = \varepsilon_{vu}$ it was taken into account. The fourth and fifth component on the right-hand side of (4) can be rearranged analogously

$$\mathrm{curl}(\vec{E}) \times \vec{D} + \vec{E}\,\mathrm{div}\,\vec{D} = \vec{i}_u\,\mathrm{div}_{|u|}(E_u\vec{D}) - \mathrm{grad}(\tfrac{1}{2}\vec{E}\vec{D}) - \vec{N}_\varepsilon + \vec{k}_\varepsilon, \tag{10}$$

$$\vec{N}_\varepsilon = -\tfrac{1}{2}E_u E_w\,\mathrm{grad}(\varepsilon_{uw}), \tag{11}$$

$$\vec{k}_\varepsilon = -\tfrac{1}{2}\frac{E_u E_w \varepsilon_{uw}}{L_{|u|}L_{|w|}}\mathrm{grad}(L_{|u|}L_{|w|}). \tag{12}$$

Equation (4) takes the form of

$$\vec{f} = -\frac{\partial}{\partial t}(\vec{D}\times\vec{B}) - \vec{i}_u \operatorname{div}_{|u|}(\vec{\vartheta}_u) + \vec{M} - \vec{N} + \vec{k}\,, \tag{13}$$

where it was defined so-called nonhomogeneous force component as follows

$$\vec{N} = \vec{N}_\mu + \vec{N}_\varepsilon\,, \tag{14}$$

and gradient

$$\vec{M} = \operatorname{grad}(\tfrac{1}{2}\vec{H}\vec{B} + \tfrac{1}{2}\vec{E}\vec{D})\,, \tag{15}$$

and ($L=L_uL_vL_w$)

$$\vec{\vartheta}_u = -H_u\vec{B} - E_u\vec{D}\,, \tag{16}$$

$$\vec{k} = \vec{k}_\varepsilon + \vec{k}_\mu + e_V \operatorname{grad}\{\ln(L)\}\,. \tag{17}$$

The relation (13) can be rewritten in the form of

$$\vec{f} = -\frac{\partial}{\partial t}(\vec{D}\times\vec{B}) - \vec{i}_u \operatorname{div}_{|u|}(\vec{\sigma}_u) + \vec{k} - \vec{N}\,. \tag{18}$$

where Maxwell stress tensor [2, 3, 4, 7] equals to

$$\vec{\sigma}_u = -H_u\vec{B} - E_u\vec{D} + \vec{i}_u e_V\,. \tag{19}$$

The equation (18) is valid for each orthogonal curvilinear co-ordinate system. It should be emphasised that the operator $\operatorname{div}_u(\ )$ in equation (7) differs from the div( ) operator and is useful for surface representation of total electromagnetic torque (see # 3.2, # 3.3).

3. ELECTROMECHANICAL CONVERTERS - LINEAR, CYLINDRICAL AND SPHERICAL

The analysis of electromagnetic field is the basis for electromechanical converter force/torque analysis. The obtained solution for magnetic field vector potential (part I) will be used for force/torque calculation.

3.1. Liner motor

Linear motors are used in electrical traction and in robotics technologies. The simplified model and dimensions thereof are presented in Fig.1.

After evaluating the magnetic field potential distribution both the magnetic flux density components and the electromagnetic torque components can be evaluated, analytically. Maxwell stress tensor leads to total electromagnetic force by means of well-known formula

$$F = \nu_o \int_{\partial V} B_\alpha B_r dS\,. \tag{20}$$

The electromagnetic force component can be evaluated by Lorentz's force density as follows

$$F_L = \int_V j_z B_r dV\,. \tag{21}$$

The difference between these two forces – called material force – is equal to

$$F_{Fe} = F - F_L\,, \tag{22}$$

and disappears due to the fact that region is homogeneous and isotropic

$$F_{Fe} = 0 . \tag{23}$$

All forces are calculated for chosen linear motor (Mathcad™ accuracy 10^{-15}) - Fig.2.

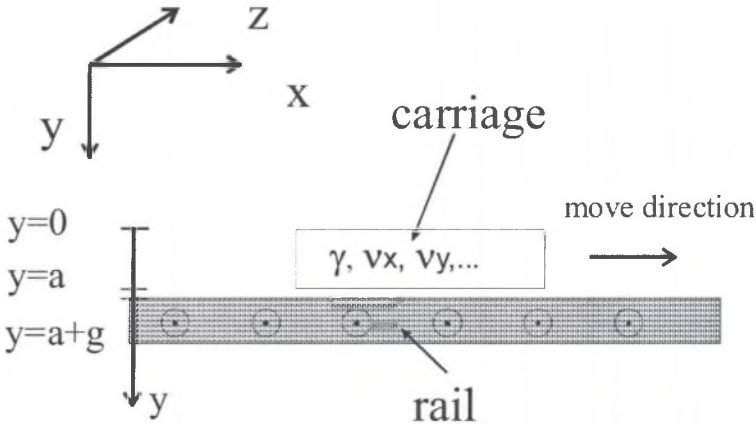

Fig. 1. Linear motor
Rys. 1. Silnik liniowy

Linear induction machine - anisotropic carriage (SI unit system)

$\nu o := 4^{-1} \cdot \pi^{-1} \cdot 10^{7}$

$\nu x := \frac{\nu o}{3}$ $\quad \nu y := \frac{\nu o}{1.2}$ $\quad \nu xy := 0.7 \cdot \nu y + 0.0 \cdot \nu y \cdot i$ $\quad \nu yx := 0.0 \cdot \nu y - 0.0 \cdot \nu y \cdot i$ $\quad \gamma := 5 \cdot 10^{6}$

$a1 := \frac{\nu yx + \nu xy}{2 \cdot \nu y} \cdot k \cdot i$ $\quad s := 2 \cdot \pi \cdot i \cdot 10$ $\quad a0 := \sqrt{k^2 \cdot \frac{\nu x}{\nu y} + \frac{\gamma \cdot s + s^2 \cdot \varepsilon}{\nu y}}$ $\quad k := 0.70$

$g := 0.005$ $\quad l := 5$ $\quad a := 0.1$ $\quad \theta s := 3000$ $\quad \lambda 1 := -a1 - \sqrt{a1^2 + a0^2}$ $\quad \lambda 2 := -a1 + \sqrt{a1^2 + a0^2}$

FORCE COMPONENTS

Maxwell method $\quad x := a + 0.3 \cdot g$

$F := l \cdot Re\left(Hy\delta(x) \cdot \overline{Bx\delta(x)}\right)$ $\quad F = 1.415$

Lorentz and material force

$F_L := Im(s) \cdot \gamma \cdot k \cdot l \cdot C$ $\quad F_L = 1.432$

$F_Fe := l \cdot k \cdot Im \int_0^a (\nu yx - \overline{\nu xy}) \cdot (Bxa(x) \cdot \overline{Bya(x)})\, dx$

Forces ratio

$\frac{F_L}{F} = 1.012$ $\quad \frac{F_Fe}{F} = -0.012$ $\quad \frac{F_L + F_Fe}{F} = 1.000$

Fig. 2. Torque calculations for anisotropic rotor - Mathcad™ program
Rys. 2. Obliczenie momentu dla anizotropowego wirnika - program Mathcad™

The electromagnetic force are calculated twice due to both Maxwell and Lorentz method – Fig.2. The relations obtained enable to discuss influence of parameters on electromagnetic force developed by electromechanical converter.

3.2. Cylindrical motor

The rotatory - cylindrically shaped induction motors are commonly used in industry. The simplified model and dimensions thereof are presented in Fig3a,b.

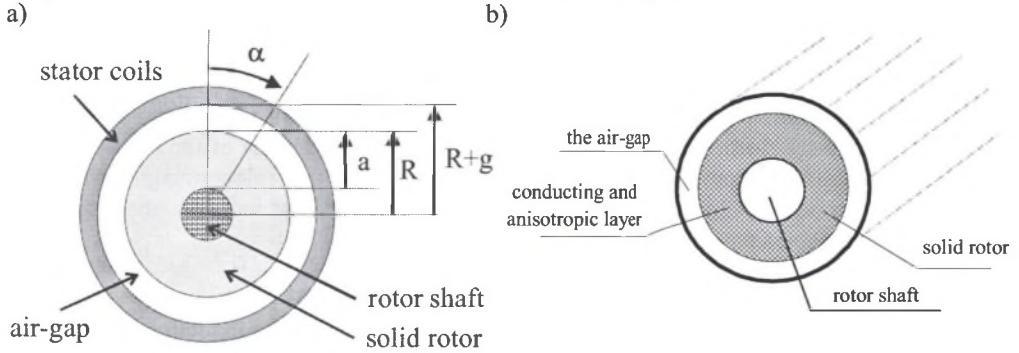

Fig. 3. Induction motor model - a) and its the cross-section and dimensions - b)
Rys. 3. Model silnika indukcyjnego - a) oraz jego przekrój poprzeczny - b)

For describing Lorentz T_{eL} and anisotropy T_{eFe} torques the proved method for induction motor with solid rotor will be applied. Let us consider the model of the induction motor with conducting and anisotropic rotor presented in Fig.3. The model can represent the 2-phase ferrite induction machine widely used in the industry. The motor rotor is magnetically homogeneous, so the tangential component of non-homogeneous component vanishes N_α=0. The magnetic rotor does not exhibit hysteresis phenomenon. The machine rotor is cylindrical. Its outer radius is R. The conducting rotor layer has the width a, and the air-gap width is g=const. The correctness of the provided analysis gives the possibility to demand for the accuracy almost of 100% for torque components values. The numerical analysis does not ensure such the level of torque calculations. The electromagnetic field calculation will be provided under the following assumptions

a) electric displacement current vanishes,

b) Maxwell's stress tensor part connected with the electric field can be omitted due to considered range of the frequency,

c) stator windings induced the sinusoidal 2p-pole magneto motive force

$$\Theta_s(\alpha) = \Theta_s\cos(p\alpha-2\pi ft), \tag{24}$$

where Θ_s stands for the magnitude of mmf, α is the position angle, f means the stator supply frequency,

d) reluctivities for motor rotor, are given by the reluctivity matrix generally.

After evaluating the magnetic field potential distribution both the magnetic flux density components and the electromagnetic torque components can be evaluated, analytically. The Maxwell stress tensor leads to the total electromagnetic torque by means of the formula

$$T_e = \nu_o r \int_{\mathcal{N}} B_\alpha B_r dS\,. \tag{25}$$

The electromagnetic torque component forced by machine rotor currents can be evaluated by Lorentz force density as follows

$$T_{eL} = \int_V r j_z B_r dV \,. \tag{26}$$

There is a question: whether the both torques are equal for electromechanical converter those rotor exhibits the magnetic anisotropy ? According to equation (18) - after applying the Gaussian theorem - for a cylindrical surface ∂V which is situated in the air-gap the difference T_{eFe} defined as follows

$$T_{eFe} = T_e - T_{eL} \,, \tag{27}$$

disappears (T_{eFe} is called material torque). The electromagnetic torques at the steady state are calculated exemplary electromechanical converter. The considered cases of the anisotropy are grouped in Table 1. For the electromechanical converter the electromagnetic torque components have been evaluated – Fig.4. There is significant that for induced anisotropy (the cases e) and g)) appears the material torque T_{eFe}.

Table 1

Rotor magnetic anisotropy cases and results of calculations for the induction motor

l= 0.3, R = 0.1, a = 0.07, Θ_s = 500, p=2, $\gamma = 7\cdot10^5$, g= 0.001, s= 2π·3.0i				
The case	**The reluctivities** $\nu_o=(4\pi10^{-7}\,H/m)^{-1}$	**Current torque ratio** $T_{e,L}/T_e$ **[%]**	**Material torque ratio** $T_{e,Fe}/T_e$ **[%]**	**Total torque value** T_e **[N·m]**
a)	$\nu_r=\nu_\alpha=0.04\nu_o$ $\nu_{r\alpha}=\nu_{\alpha r}=0$	100,0	0,0	4,29
b)	$\nu_\alpha=0.04\nu_o$ $\nu_r=0.05\nu_o$ $\nu_{r\alpha}=\nu_{\alpha r}=0$	100,0	0,0	3,46
c)	$\nu_r=\nu_\alpha=0.04\nu_o$ $\nu_{r\alpha}=\nu_{\alpha r}=0.1\nu_r$	100,0	0,0	4,34
d)	$\nu_\alpha=0.04\nu_o$ $\nu_r=0.05\nu_o$ $\nu_{r\alpha}=\nu_{\alpha r}=0.1\nu_r$	100,0	0,0	3,50
e)	$\boldsymbol{\nu_\alpha=0.04\nu_o}$ $\boldsymbol{\nu_r=0.05\nu_o}$ $\boldsymbol{\nu_{r\alpha}=0.10\nu_r}$ $\boldsymbol{\nu_{\alpha r}=0.15\nu_r}$	**91,4**	**8,6**	**3,83**
f)	$\nu_\alpha=0.04\nu_o$ $\nu_r=0.05\nu_o$ $\nu_{r\alpha}=-0.10i\nu_r$ $\nu_{\alpha r}=+0.10i\nu_r$	100,0	0,0	4,01
g)	$\boldsymbol{\nu_\alpha=0.04\nu_o}$ $\boldsymbol{\nu_r=0.05\nu_o}$ $\boldsymbol{\nu_{r\alpha}=\{0.10-i0.10\}\nu_r}$ $\boldsymbol{\nu_{\alpha r}=\{0.15+i0.10\}\nu_r}$	**91,3**	**8,7**	**4,44**

From the analyses carried out and grouped in Table 1 it is apparent, that *the material torque component disappears for induction motor with round, homogeneous and non-hysteresis rotor if the matrix of magnetic reluctivities is Hermitan conjugate one.*

Hence, *there is possible to express the total torque T_e (calculated by Maxwell stress surface integral) caused by Lorentz force in the form of surface integral for Hermitian conjugate reluctivity matrix.*

For the analysis of influence of normal magnetic anisotropy ($\mu_{r\alpha} = \mu_{\alpha r} = 0$) on torque-slip curve shape there are considered three cases of rotor magnetic anisotropy

with radial-dominate magnetic reluctivity - Tr and $\mu_r > \mu_\alpha$,

with angular-dominate magnetic reluctivity - Tα and $\mu_\alpha > \mu_r$,

compared with the case of isotropic rotor – T0.

For the three specified above cases (at condition $\mu_r + \mu_\alpha = \text{const} = 30\cdot\mu_o$, $\gamma = 7\cdot10^6$ S/m, R=0.05m, a=0.03m, g=0.001m, Θ=500A, p=1, l=0.3m, f_l=50Hz) the electromagnetic steady-state torque-slip curve ($s=(f_l-np)/f_l$) have been obtained with the help of the presented magnetic field distribution - Fig.5.

Induction motor with solic anisotropic rotor

$\nu r := \frac{\nu o}{20}$ $\nu\alpha := \frac{\nu o}{25}$ $\nu r\delta := \nu o$ $\nu\alpha\delta := \nu o$ $\nu r\alpha := 0.1\cdot\nu\alpha$ $\nu\alpha r := 0.15\cdot\nu\alpha$

$c := \frac{\nu\alpha r + \nu r\alpha}{2\cdot\nu\alpha}\cdot p\cdot i$ $s := 2\cdot\pi\cdot i\cdot 3$ $pB := \sqrt{p^2\cdot\frac{\nu r}{\nu\alpha} + c^2}$ $p\delta := p\cdot\sqrt{\frac{\nu r\delta}{\nu\alpha\delta}}$ $p := 2$

$g := 0.001$ $l := 0.3$ $R := 0.1$ $a := 0.07$ $\theta s := 500$ $\gamma := 7\cdot10^6$

$c = -0.25i$ $pB = 2.222$ $\beta := \sqrt{(s\cdot\gamma + s^2\cdot\varepsilon)\cdot\nu\alpha^{-1}}$ $\beta o := \sqrt{s\cdot\gamma\cdot\nu\alpha^{-1}}$

$|\beta\cdot(R-a)| = 1.932$ $|\beta\cdot R| = 6.438$

Torque components $r := R + 0.5\cdot g$

Maxwell method:

$Tc := r^2\cdot\pi\cdot l\cdot Re(H\alpha\delta(r)\cdot\overline{Br\delta(r)})$ $Tc = 5.454$

Lorentz and material torques:

$TeL := p\cdot\pi\cdot l\cdot Im(s)\cdot\gamma\cdot\int_{Ra}^{R}(|Aa(r)|)^2\cdot r\,dr$ $TeL = 5.391$

$TeFe := p\cdot\pi\cdot l\cdot Im\int_{Ra}^{R}(\nu\alpha r - \overline{\nu r\alpha})\cdot(Bra(r)\cdot\overline{B\alpha a(r)})\cdot r\,dr$ $TeFe = 0.063$

Torques ratios:

$\frac{TeL}{Te} = 0.98836$ $\frac{TeFe}{Te} = 0.01164$ $\frac{TeL + TeFe}{Te} = 1.00000$

Fig. 4. Torque calculations for anisotropic rotor - Mathcad™ program

Rys. 4. Moment elektromagnetyczny dla silnika o wirniku anizotropowym - program Mathcad™

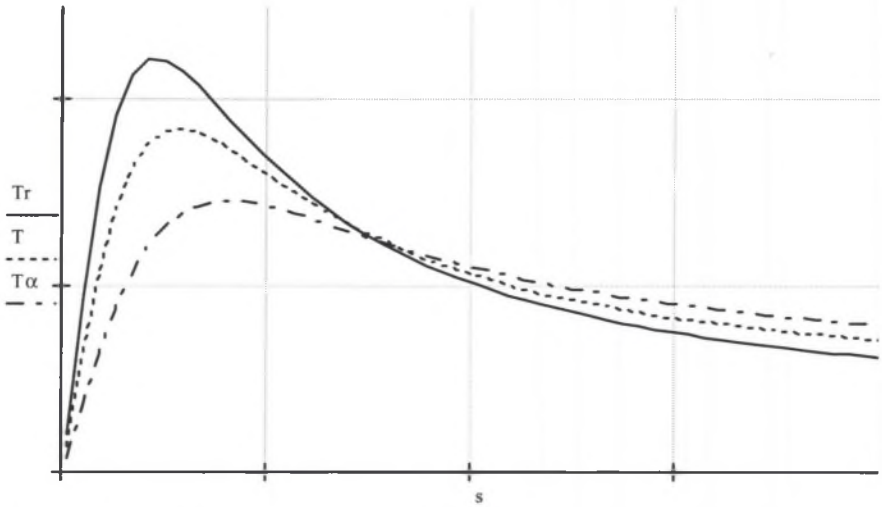

Fig. 5. Torque-slip curves for different anisotropy: Tr for $\mu_r > \mu_\alpha$ - solid line, T for $\mu_r = \mu_\alpha$ - dot line (isotropic rotor), Tα $\mu_r > \mu_\alpha$ - dash-dot line (for all cases $\mu_r + \mu_\alpha = \text{const}$, $\mu_{r\alpha} = \mu_{\alpha r} = 0$)

Rys. 5. Charakterystyka mechaniczna dla różnych przypadków anizotropii: Tr dla $\mu_r > \mu_\alpha$ - linia ciągła, T dla $\mu_r = \mu_\alpha$ - linia kropkowana (izotropowy wirnik), Tα $\mu_r > \mu_\alpha$ - linia kropka-kreska ($\mu_r + \mu_\alpha = \text{const}$, $\mu_{r\alpha} = \mu_{\alpha r} = 0$)

The analyses carried for cylindrically shaped electromechanical converter have brought out to the issues, such as

- For the electromechanical converter with round rotor, which does not exhibit both the nonhomogenity of magnetic reluctivity and the hysteresis phenomenon only the anisotropy of the magnetic reluctivity may cause the material torque. Indeed, the material torque appears for the cylindrical-shaped electromechanical converter as it was shown above in the case

$$\nu_{r\alpha} \neq \overline{\nu}_{\alpha r}$$

- For the electrical machine rotor with radial-dominate magnetic reluctivity the electromagnetic torque is the greatest one for stable part of torque-slip curve.
- The obtained results enable one to state that the electromagnetic torque of electromechanical converter can be represented by the surface integral for both the isotropic and the normal magnetic anisotropy of rotor.

3.3. Spherical motor

Spherically shaped motors are used in robotics technologies and as actuators [3, 5, 6, 10]. The simplified model and dimensions thereof are presented in Fig.6a,b and dimensions in Fig. 3b. (as for the cylindrical motor)

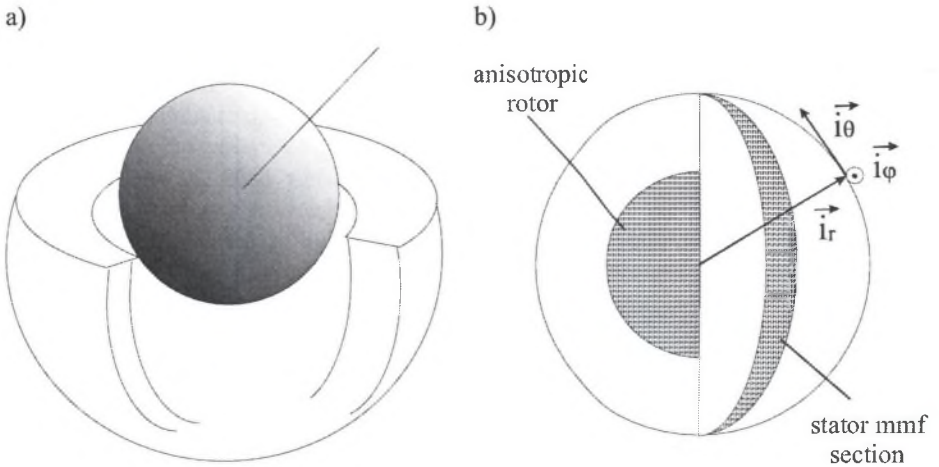

Fig. 6. Spherically shaped electromechanical converter - a) its cross section view -b)
Rys. 6. Przetwornik elektromechaniczny o symetrii sferycznej - a) przekrój poprzeczny -b)

The analytical solution for the spherical motor can be presented in terms of separated function R(r) and F(φ,θ) obtained with the help of separation proposed. The exemplary spherical induction motor with anisotropic and spherical rotor is considered. For the monoharmonic magnetomotive force of stator [1] the magnetic field distribution and electromagnetic torque are calculated. The data for analysis are presented in Fig.7.

Spherical induction motor with anisotropic rotor (SI units)

$$\nu r := \frac{\nu o}{5} \quad \nu\phi := \frac{\nu o}{10} \quad \nu r\delta := \frac{\nu o}{2} \quad \nu\phi\delta := \frac{\nu o}{3} \quad \nu r\phi := 0.3\cdot\nu\phi \quad \nu\phi r := 0.3\cdot\nu\phi \quad p := 1$$

$$h := z\frac{\nu\phi r + \nu r\phi}{2\cdot\nu\phi}\cdot p\cdot i \quad \lambda 1 := \sqrt{(0.5-h)^2 + \left(\nu r\cdot p^2 + z\cdot p\cdot i\cdot\nu r\phi\right)\cdot\nu\phi^{-1}} \quad \lambda 2 := -\lambda 1 \quad \lambda := \lambda 1 \quad s := 2\cdot\pi\cdot i\cdot 10$$

$$g := 0.002 \quad R := 0.05 \quad a := 0.03 \quad \theta s := 5000 \quad \gamma := 7\cdot 10^6 \quad \lambda = 1.46969$$

Fig. 7. The data set for the exemplary spherical motor
Rys. 7. Parametry geometryczne i środowiskowe przykładowego silnika sferycznego

For the evaluated magnetic filed distribution and electromagnetic torque has been calculated as shown in Fig.8. There are presented the electromagnetic torques two components: Lorentz T_{eL} and material T_{eFe} that together constitute the total electromagnetic torque T_e. This is presented for checking of the calculations correctness. It should be pointed out that for either isotropic or normally anisotropic ($\nu_{\varphi r}=\nu_{r\varphi}$) rotor the material torque component disappears (generally for Hermite-conjugate reluctivity matrix). The condition for is the same as for cylindrically shaped rotor (# 3.2).

Electromagnetic torque - total value

$r := R + 0.6 \cdot g$

Maxwell's method

$Te := r^3 \cdot \pi \cdot I\theta \cdot Re\left(H\phi\delta(r) \cdot \overline{Br\delta(r)}\right)$

$Te = 0.055$

Lorentz and material torques

$TeCu := -z \cdot p \cdot \pi \cdot \gamma \cdot I\theta \cdot Im(s) \cdot Cr$ $\quad TeCu = 0.055$

$$TeFe := p \cdot \pi \cdot I\theta \cdot Im \int_{Ra}^{R} \left(v\phi r - \overline{vr\phi}\right) \cdot \left(Bra(r) \cdot \overline{B\phi a(r)}\right) \cdot r^2 \, dr$$

Torques ratios

$\frac{TeCu}{Te} = 1.000$ $\quad \frac{TeFe}{Te} = 0.000$ $\quad \frac{TeCu + TeFe}{Te} = 1.00000$

Fig. 8. Electromagnetic torque calculation for spherical motor
Rys. 8. Obliczenie momentu elektromagnetycznego dla silnika o symetrii sferycznej

In order to check the accuracy of electromagnetic field solutions the energy-power balance has been checked. The Poynting vector is used for evaluating the magnetic energy and power losses in rotor. The part of exemplary calculations are shown in Fig.9. For checking the correctness of the obtained electromagnetic field distribution the power balance has been checked with the help of MathCad™ program. The complex power is calculated with the help of Poynting vector as follows

$$S_c = -i\omega v_o \int_S B_{\varphi\delta} A_z dS \,. \tag{28}$$

The fulfilment of electromagnetic field power balance ensures us that the analytical solutions are correct. Moreover, the power analysis leads to the power losses value in solid rotor

$$P_q = \gamma \int_V E_z^2 dV \,, \tag{29}$$

that are very important from thermal point of view [6].

Magnetic field energy stored

$$Ia := \begin{cases} 0 & \text{if } (vr\phi = 0) \cdot (v\phi r = 0) \\ 0.5 \cdot k \cdot \int_{Ra}^{R} Bra(r) \cdot \overline{B\phi a(r)} \cdot r^2 \, dr & \text{otherwise} \end{cases}$$

$$Er := \frac{\overline{vr}}{2} \cdot k \cdot \int_{Ra}^{R} \left(|Bra(r) \cdot r|\right)^2 dr \qquad Io := \int_{Ra}^{R} r^2 \cdot \left(|Aa(r)|\right)^2 dr$$

$$E\phi := \frac{\overline{v\phi}}{2} \cdot k \cdot \int_{Ra}^{R} \left(|B\phi a(r)|\right)^2 \cdot r^2 \, dr$$

$E\phi r := \overline{vr\phi} \cdot Ia \qquad E\phi r := \overline{v\phi r} \cdot \overline{Ia}$

Electric field energy stored

$E\mu := Er + E\phi + E\phi r + E\phi r$

$E\varepsilon := 0.5 \cdot \varepsilon \cdot k \cdot (|s|)^2 \cdot Io$ $\quad E\varepsilon = 0$

Active power

$E\mu = 0$

Reactive power

$Pq := (|s|)^2 \cdot \gamma \cdot k \cdot Io$ $\quad Pq = 0.018$

Complex power

$Q := 2 \cdot Im\left(s \cdot E\mu + \overline{s} \cdot E\varepsilon\right)$ $\quad Q = 0.021$

$Pe := 2 \cdot Re\left(s \cdot E\mu + \overline{s} \cdot E\varepsilon\right)$ $\quad Pe = 0$

$Sc := -v\phi\delta \cdot k \cdot R^2 \cdot s \cdot A\delta(R) \cdot \overline{B\phi\delta(R)}$

$Sc = 0.018 + 0.021i$

$\frac{E\phi r + E\phi r}{Er + E\phi} = 0.001$ $\quad \frac{E\varepsilon}{E\mu} = 0.000$ $\quad \frac{Pq + Pe + Q \cdot i}{Sc} = 1.00000$

Fig. 9. Electromagnetic field energy balance – calculation (program extract)
Rys. 9. Bilans energii pola elektromagnetycznego – obliczenia (fragment programu)

For the analysis of influence of normal magnetic anisotropy ($\mu_{r\varphi} = \mu_{\varphi r} = 0$) on torque-slip curve there are considered three cases of rotor magnetic anisotropy

with radial-dominate magnetic reluctivity - Tr and $\mu_r > \mu_\varphi$,

with angular-dominate magnetic reluctivity - Tϕ and $\mu_\varphi > \mu_r$,

compared with the case of isotropic rotor – T.

For the three specified above cases (at condition $\mu_r + \mu_\varphi = \text{const} = 30 \cdot \mu_o$, $\gamma = 7 \cdot 10^6$ S/m, R=0.05m, a=0.03m, g=0.002m, Θ=1000A, p=1 – the radii are as in Fig.3) the electromagnetic steady-state torque-slip curve have been obtained with the help of the presented magnetic field distribution - Fig.10. The torque-slip curves show that electromechanical converter with radial-dominate magnetic reluctivity develops electromagnetic torque at stable part of torque-slip curve greater than for other anisotropy and isotropic rotor.

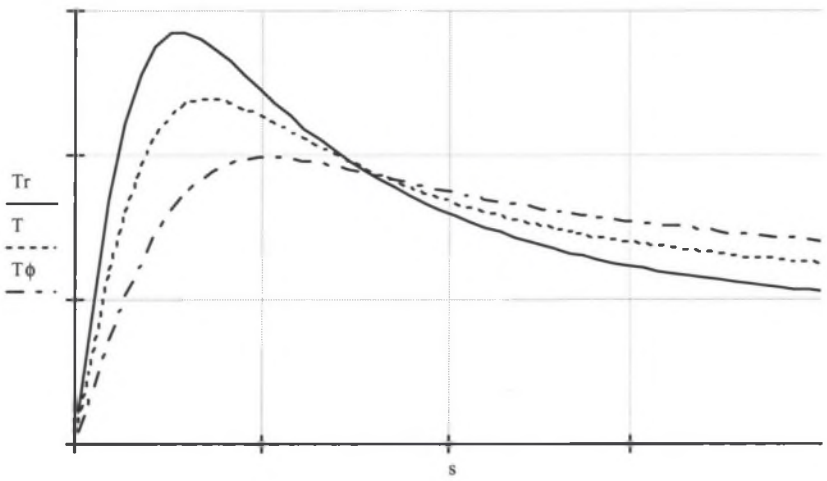

Fig. 10. Torque-slip curves for different anisotropy: Tr for $\mu_r > \mu_\varphi$ - solid line, T for $\mu_r = \mu_\varphi$ - dot line (isotropic rotor), Tϕ for $\mu_r > \mu_\varphi$ - dash-dot line (for all cases $\mu_r + \mu_\varphi = \text{const}$, $\mu_{r\varphi} = \mu_{\varphi r} = 0$) for spherical motor

Rys. 10. Charakterystyka mechaniczna dla różnych przypadków anizotropii: Tr dla $\mu_r > \mu_\varphi$ - linia ciągła, T dla $\mu_r = \mu_\varphi$ - linia kropkowa (izotropowy wirnik), Tϕ dla $\mu_r > \mu_\varphi$ - linia kropka-kreska ($\mu_r + \mu_\varphi = \text{const}$, $\mu_{r\varphi} = \mu_{\varphi r} = 0$)

4. CONCLUSIONS

The paper presents electromagnetic force/torque calculation described in analytical way enables to calculate total and its components values. The force/torque components indicate the physical reason for theirs induction i.e. Lorentz force and material force component (here anisotropy features).

The mathematical prove for the main equation (18) for force density has been provided. The operator definition (7) is convenient due to its mathematical form not only for curvilinear co-ordinate system but also for calculations.

For the chosen electromechanical converters linear, cylindrical and spherically shaped electromagnetic field and force/torque have been calculated. The accuracy of the calculation carried out has been checked by total force/torque decomposition correctness, too.

The parameters influence analysis on force/torque values leads to the conclusions that the radial-dominate anisotropy increases the electromagnetic torque value at steady-state (#3.2, #3.3).

For spherically shaped electromechanical converter the non-standard separation is proposed that leads to the analytical solutions. The mathematical form of non-standard separation is given in part I.

It is pointed out the fact that the Lorentz force can be presented by means of surface integral for isotropic and anisotropic regions for Hermite-conjugate symmetry for reluctivity matrix.

REFERENCES

1. Adkins B., Harley P.G.: *The general theory of alternating current machines*. Chapman and Hall, London 1978.
2. Bolte E., Hahlweg C.: *Analysis of steady-state of high speed induction motors with exterior rotor and conductive layer on the slotted stator*. Proceedinds of XV ICEM , Belgium, 2002.
3. Davey K., Vachtsevanos G., Powers R.: *The analysis of fields and torques in spherical induction motors*. „IEEE Transaction on Magnetics" 1987, Vol. Mag-23, No. 1.
4. Demenko A.: *Finite element analysis of electromagnetic torque saturation harmonics in a squirrel cage machine*. COMPEL 1999, Vol. 18, No.4, p.619-628.
5. Kamiński G.: *Electric motors with rolling rotors (Silniki elektryczne z toczacymi sie wirnikami - in Polish*), Wyd. Politechnika Warszawska, Warszawa 2003.
6. Purczyński J., Kaszycki L.: *Power losses and electromagnetic torque of spherical induction motor (Straty mocy i moment napędowy silnika indukcyjnego o symetrii kulistej - in Polish)*. „Rozprawy Elektrotechniczne" 1988, Vol. 34, z.3, p.819-838
7. Spałek D.: *Electromagnetic torque components in synchronous salient-pole machine*. „The International Journal for Computation & Mathematics in Electrical & Electronics Engineering COMPEL" 1997, Vol. 16, Issue 3, MCB UK, p.129-143.
8. Spałek D.: *Anisotropy component of electromagnetic torque in electrical machines*. „Archives of Electrical Engineering" 1999, No 1, p. 109-126.
9. Spałek D.: *Fast analytical model of induction motor for approaching rotor eccentricity*. „COMPEL International Journal for Computation Mathematics in Electrical & Electronics Engineering" 1999, Vol. 18, Issue 4, p. 570-586, MCB University Press, UK.
10. Zhou, Z. and Lee, K.-M.: *Characterization Of A Three Degrees-Of-Freedom Variable-Reluctance Spherical Motor*. „Journal Of Systems Engineering" (Special Issue on Motion Control) 1994, Vol. 4, p. 60-69.

Recenzent: Prof. dr hab. inż. Stanisław Wincenciak

Wpłynęło do Redakcji dnia 14 kwietnia 2004 r.